

## ARTÍCULOS

**Tree carbon stock in evergreen forests of Chiloé, Chile**

Reservorio de carbono arbóreo en bosques siempreverdes de Chiloé, Chile

**Jorge F Perez-Quezada <sup>a,b\*</sup>, Sebastián Olguín <sup>a</sup>, Juan P Fuentes <sup>c</sup>, Mauricio Galleguillos <sup>a</sup>**\*Corresponding author: <sup>a</sup> Universidad de Chile, Facultad de Ciencias Agronómicas, Casilla 1004, Santiago, Chile, tel.: 56-2-29785840, jorgepq@uchile.cl<sup>b</sup> Instituto de Ecología y Biodiversidad, Santiago, Chile<sup>c</sup> Universidad de Chile, Facultad de Ciencias Forestales y de la Conservación de la Naturaleza, Santiago, Chile.

## SUMMARY

The carbon stock associated with tree biomass was estimated in evergreen forests near the town of Iníó in Chiloé Island, Chile (43°21' S, 74°07' W), analyzing its relation with biotic and abiotic properties. A total of 14 sampling plots of 20×50 m were located at variable distances from Iníó and different elevations, slopes and aspects. At each plot, tree density, incident solar radiation, and spectral vegetation indices were quantified based on LANDSAT satellite data. Total tree carbon stock was estimated for each tree species and in total, using known allometric biomass functions based on the diameter at breast height (DBH), of all the trees in the plot with DBH > 3 cm. Four plots presented post-fire conditions, where tree carbon content had a mean ( $\pm$  SE)  $7.7 \pm 0.78$  Mg ha<sup>-1</sup>, while in the unburned plots it was  $384.4 \pm 120$  Mg ha<sup>-1</sup>. After removing the value of one plot with high carbon content, the average was  $189.7 \pm 45.6$  Mg ha<sup>-1</sup>. Most of the sampled properties had a limited correlation with tree carbon content ( $R^2$  0.31-0.69). However, the amount of carbon of *Nothofagus nitida* was related to the total tree carbon in all the plots (post-fire and unburned) with  $R^2 = 0.96$ . This model substantially simplifies sampling efforts, since only DBH data of *N. nitida* is needed for the analyses (average of 15 individuals per plot). The tree carbon stock of forests of this area is high when compared to other forest types of the world.

*Key words:* carbon pool, biotic and abiotic variables, *Nothofagus nitida*, allometric models.

## RESUMEN

El reservorio de carbono asociado a la biomasa arbórea fue estimada en bosques siempreverdes cerca de Iníó en la isla de Chiloé, Chile (43°21' S, 74°07' O), analizando su relación con propiedades bióticas y abióticas. Un total de 14 parcelas de 20×50 m fueron ubicadas a distancias variables de Iníó y diferentes altitudes y pendientes. Para cada parcela, también se cuantificó la densidad total de árboles, radiación solar incidente e índices espectrales de vegetación basados en datos satelitales LANDSAT. El reservorio de carbono en los árboles por especie y total fue estimado usando funciones alométricas conocidas, basadas en el diámetro a la altura del pecho (DAP), de todos los árboles de cada parcela con DAP > 3 cm. Cuatro parcelas presentaron una condición post-incendio, donde el contenido de carbono arbóreo promedio ( $\pm$  EE) fue de  $7,7 \pm 0,78$  Mg ha<sup>-1</sup>, mientras que en las áreas no incendiadas fue de  $384,4 \pm 120$  Mg ha<sup>-1</sup>. Después de remover una parcela con contenido de carbono alto, el promedio fue de  $189,7 \pm 45,6$  Mg ha<sup>-1</sup>. La mayor parte de las variables muestreadas tuvieron una correlación limitada con el contenido de carbono arbóreo ( $R^2$  0,31-0,69). Sin embargo, la cantidad de carbono de *Nothofagus nitida* se relacionó con el total de carbono arbóreo en todas las parcelas (post-incendio y no incendiadas) con un  $R^2 = 0,96$ . Este modelo simplifica el esfuerzo de muestreo sustancialmente, ya que solo requiere los datos de DAP de *N. nitida* para el análisis (promedio de 15 individuos por parcela). El reservorio de carbono arbóreo de bosques maduros en esta área es alto en comparación con otros tipos de bosque del mundo.

*Palabras clave:* reservorio de carbono, variables bióticas y abióticas, *Nothofagus nitida*, modelos alométricos.

## INTRODUCTION

Atmospheric carbon dioxide (CO<sub>2</sub>) concentration increased from 280 ppm (pre-industrial times) to 379 ppm in 2005, whereas the increase in the preceding 8,000 years of the industrial revolution was only 20 ppm (IPCC 2007). The general increase in greenhouse gases is the result of

several factors including demographic growth, socio-economical development and changes in technology (Metz *et al.* 2005). Atmospheric CO<sub>2</sub> increase is attributed to global fossil fuel consumption and to the effect of land use change on soils and plants (IPCC 2007).

Deforestation is defined as the long-term or permanent removal of the forest cover in which land use change is

considered a primary cause (IPCC 2000). The decrease in vegetation implies both an immediate increase and a gradual increase (depending on the final destiny of the logged biomass) in carbon emissions to the atmosphere, as well as a decrease in vegetation cover available for sequestering carbon. Forest ecosystems are the main terrestrial carbon reservoir, as well as the ecosystems with the greatest exchange of carbon between the atmosphere and the soil (Kim Phat *et al.* 2004). The amount of carbon in these ecosystems varies as a function of the biome, forest type and the compartment being analyzed (*i.e.*, tree vegetation, necromass, litter layers, soil) (Ajtay *et al.* 1979) and the development stage (Gutiérrez and Huth 2012).

The potential carbon sequestration of forest ecosystems can be directly determined by using methods that evaluate carbon fluxes at canopy scale in a short period of time, such as eddy covariance and Bowen ratio techniques (Moncrieff *et al.* 2000). Nevertheless, such methods are expensive and difficult to be implemented. Another less expensive approach is the comparison of carbon stocks in different times (Goodale *et al.* 2002, Schulp *et al.* 2008). In the case of forest ecosystems, the carbon able to be stored is a function of prevailing environmental conditions (*e.g.* precipitation, vapor pressure deficit, elevation, slope, aspect, soil chemical and physical properties, soil morphology) and natural disturbance regimes (Keith *et al.* 2009). The effect of tree species has also been reported as a significant factor controlling soil carbon stocks in temperate and boreal forests (Vesterdal *et al.* 2013). The methods and working scales used for carbon estimation of forest ecosystems are diverse. The most common approach used is the forest inventory, which constitutes the basis for the application of statistical models for estimating above and below-ground biomass. The main restriction of this approach is its high cost, particularly when used in large areas (Brown 2002); therefore it is usually complemented with remote sensing techniques and modeling, integrated to geographic information systems that allow estimations at larger spatial scales (Spencer *et al.* 1997, Lu 2006, Zheng *et al.* 2007).

The forests of Chiloé differ from similar continental forests due to a particular combination of more hygrophytic plant species in which the Myrtaceae family dominates (Villagrán *et al.* 1986). In addition, Chiloé forests are of particular interest due to the confluence of floristic elements from both the Valdivian (*e.g.* *Aetoxicon punctatum* (Ruiz *et Pav.*), *Amomyrtus meli* (Phil.) D. Legrand *et Kausel*) and subantarctic (*e.g.* *Euphrasia antarctica*, *Pratia repens*, *Deschampsia laxa*) forests (Villagrán *et al.* 1986). Historically, extensive areas of native forest ecosystems of Chile have been altered by human activities (*e.g.*, forest fires, land use change, selective tree cutting) (Altamirano and Lara 2010, Castillo *et al.* 2012). In this regard, the southern part of Chiloé Island was declared a priority site for conservation of biodiversity (Chaiguata Priority Site) by the National Commission of Environment, also

because it is the habitat of the largest population of *Lontra provocax* (Southern river otter) and many amphibian species (CONAMA 2002). Although this area possesses high species diversity, their forest ecosystems are not well represented in the National Wildlife Protection System of the Chilean State (SNASPE) (Squeo *et al.* 2012). Private initiatives have counterbalanced this lack of representation, creating a relatively new conservation park: Tantauco. This park includes an important extension of the Chaiguata Priority Site, in which pristine forest ecosystems as well as burned and logged forests are found. This mosaic of forest patches with different structural characteristics has not been evaluated in terms of their actual carbon stocks.

Given the ecological importance of these types of forests and the lack of information about the amount of carbon stored in these ecosystems, we hypothesized that carbon estimations can be developed from topographic and satellite spectral parameters, considering also the anthropogenic influence in the landscape (*i.e.*, closeness of forests to human populated areas). We aimed at: 1) measuring the carbon stock of coihue de Chiloé (*Nothofagus betuloides*)-tepa (*Laureliopsis philippiana*) forest stands and, 2) determining the relationship between biotic (*e.g.* tree density) and abiotic variables (*e.g.* elevation, solar radiation, spectral parameters) with the amount of tree carbon. These two objectives were accomplished by installing a set of plots near the village of Iníó, where abiotic characteristics and vegetation structure data were collected. The tree carbon stock was determined using individual biomass functions (tree biomass as a function of its diameter) that were applied to density data of each plot. Carbon stocks were then correlated to the abiotic and biotic parameters.

## METHODS

**Study area.** The study was conducted in Tantauco Park, located in the southern end of Chiloé Island (figure 1), which has a total area of 118,000 ha. The study area was near the village of Iníó (43°21'45''S, 74°07'16''W). Elevations in the park range from 0 to 100 m a.s.l. in 77 % of the area, and between 100 and 300 m a.s.l. in the rest of the area. Approximately 95 % of the park has slopes lower than 34.4 %. Some specific locations with slopes higher than 66.4 % are possible to be found (Corporación Chile Ambiente 2005). Air temperatures vary between -2 and 27 °C, and mean annual precipitation is about 3000 mm (Corporación Chile Ambiente 2005).

According to Gajardo (1994), the vegetation in the study area is classified as Evergreen Forests and Wetlands. According to Corporación Chile Ambiente (2005) and using Cajander's forest type classification (Cajander 1926, Donoso 1981), the most representative forest type of the area is Chiloé coihue (*Nothofagus nitida* (Phil.) Krasser) -tepa (*Laureliopsis philippiana* (Looser) Schodde), which covers about 31.4 % of the area (37,000 ha). Accompan-

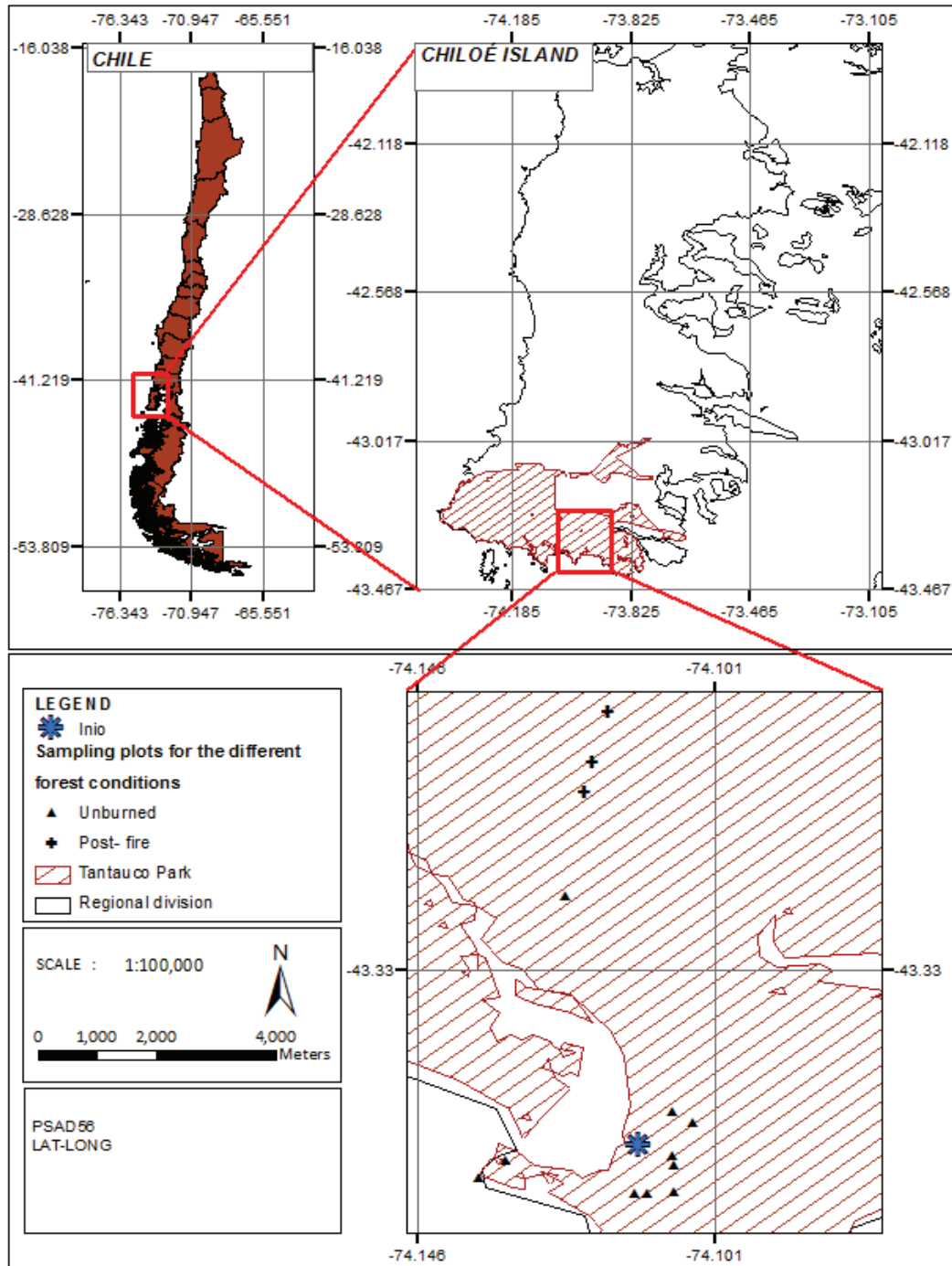


**Figure 1.** Location of the sampling plots at the Tantauco Park in Chiloé Island.

Ubicación de los sitios de muestreo en el Parque Tantauco, en la Isla de Chiloé.

ying flora in this forest type is canelo (*Drimys winteri* J.R. Forst. et G. Forst.) and tiaca (*Caldcluvia paniculata* (Cav.) D. Don). The dominant soil texture is silty clay loam, with high organic matter content (22-38 % in the first 20 cm). Fertility is low, but Chiloé coihue-tepa forest type generally dominates in soils that are humid and have higher fertility (Corporación Chile Ambiente 2005).

A total of 14 sampling plots of 1,000 m<sup>2</sup> (20×50 m) were located to capture the variability of the abiotic properties elevation, slope, aspect and distance from Iníó village. We expected the distance from human population to show the magnitude of perturbation, *i.e.*, the closer to Iníó (located by the ocean), the higher the perturbation of forest ecosystems and the lower the tree biomass.

*Estimation of live tree carbon stock.* In each plot, the diameter at breast height (DBH) of all live trees (DBH > 3 cm) was measured. Aboveground tree biomass was estimated using allometric functions developed by Gayoso *et al.* (2002), which estimate tree biomass (kg) based on DBH, for five species present in our study (*N. nitida*, *D. winteri*, *L. philippiana*, *tineo* (*Weinmannia trichosperma* (Cav.)), and mañío macho (*Podocarpus nubigenus* Lindl.) (table 1). For the rest of the species or trees with DBH outside the range of the specific functions, we used a general biomass function for the evergreen forest of the Coastal Mountain Range of Chile (Gayoso *et al.* 2002) (table 1).

For the estimation of belowground biomass (*i.e.* tree roots), we followed the aboveground/belowground biomass ratios determined by Gayoso *et al.* (2002) specifically reported for five species of our study, and a mean conversion value of 28.69% for the rest of the species (table 1). In order to transform above and belowground tree biomass to carbon weight, we used the conversion values estimated by Gayoso *et al.* (2002) (table 1). These conversion values ranged between 43 and 46 %, which are lower than the 50 % proposed as a standard by IPCC (1996). The total carbon content from the tree biomass reservoir was estimated by adding together the above and belowground biomass.

*Sampling and calculation of biotic and abiotic properties.* Among the abiotic properties, elevation, slope and aspect were directly obtained from a 30 m ground resolution ASTER GDEM, Digital Elevation Model, freely available at <http://www.gdem.aster.ersdac.or.jp/>. Potential global solar radiation ( $\text{kW h}^{-1} \text{m}^{-2}$ ) was computed with the 'solar analysis' tool of the ArcGIS 10.1 software (ESRI, USA). This tool is able to map potential solar global radiation as

a function of the solar constant, day length, latitude, longitude, slope and aspect, using a digital elevation model (DEM). The radiation value was calculated for each day of the year, estimating then the annual radiation in  $\text{MJ m}^{-2} \text{year}^{-1}$ . Northing, which is the linearization of the aspect, was defined as the  $\cos(\text{aspect} \cdot \pi / 180)$ . The variable 'distance to Inío' was estimated using algorithms of the ArcGIS 10.1 software; determining the central points of each sampling plot and the center of Inío village as the origin. For the calculation of spectral variables, we used the normalized vegetation index (NDVI, Rouse *et al.* 1973), the corrected normalized vegetation index (NDVIC, Nemani *et al.* 1993) and the red green index (GreenIndex, Coops *et al.* 2006). Additionally, the Tasseled cup transformation (Crist and Cicone 1984) was computed, since it allows the use of spectral information obtained from the visible, near-infrared, and medium-infrared spectra of the LANDSAT ETM+ satellite sensor. Greenness, Wetness, and Brightness indices were obtained with the Tasseled cup transformation (Kauth and Thomas 1976). All indices were calculated from two scenes captured on February 2 and 18 of 2008 with 30 m of ground spatial resolution. Radiometric and atmospheric corrections of the LANDSAT images (Chavez 1988) were made previous to estimating the indices. The coefficients used for calculating reflectance were obtained from the study of Chander *et al.* (2009). To correct the SLC-off error, both images were fused using the method of Scaramuzza *et al.* 2004. The reflectance bands were also used to obtain the Tasseled Cap transformation and the vegetation indices. Satellite image processing was made with the ENVI 5.0 software. The biotic properties sampled were total tree density and the carbon content associated with individual tree species that were found in all plots.

**Table 1.** Specific and general equations of aboveground biomass ( $B_{ab}$ ) as a function of diameter at breast height (DBH) and the percentage of belowground biomass, for tree species of the evergreen forest of the Coastal Mountain Range of Chile, from Gayoso *et al.* (2002).

Ecuaciones de biomasa aérea generales y específicas en función del diámetro a la altura del pecho (DBH) y el porcentaje de biomasa subterránea, de Gayoso *et al.* (2002).

Tree species	Function	DBH (cm)	Adj- R <sup>2</sup>	B <sub>b</sub> <sup>a</sup> (%)	C <sub>a</sub> <sup>b</sup> (%)	C <sub>b</sub> <sup>c</sup> (%)
<i>N. nitida</i>	$B_{ab} = -146.92 + e^{(4.76 + 0.05 \times \text{DBH})}$	12 - 47	0.98	24.15	44.55	43.75
<i>D. winteri</i>	$B_{ab} = -5.73 + e^{(3.25 + 0.07 \times \text{DBH})}$	6 - 52	0.97	21.84	45.49	44.69
<i>L. philippiana</i>	$B_{ab} = e^{(-0.88 + 2.00 \times \text{LN}(\text{DBH}))}$	6 - 74	0.95	-	-	-
<i>W. trichosperma</i>	$B_{ab} = -170.11 + e^{(5.23 + 0.03 \times \text{DBH})}$	6 - 91	0.97	-	-	-
<i>P. nubigena</i>	$B_{ab} = e^{(-0.22 + 1.77 \times \text{LN}(\text{DBH}))}$	7 - 54	0.99	29.38	45.89	44.07
Any tree	$B_{ab} = e^{(2.08 + 0.15 \times \text{DBH})}$	< 20 cm	0.77	28.69	44.06	45.03
Any tree	$B_{ab} = e^{(4.48 + 0.05 \times \text{DBH})}$	> 20 cm	0.76	28.69	44.06	45.03

<sup>a</sup> Belowground biomass as a percentage of aboveground biomass.

<sup>b</sup> Percentage of carbon in aboveground biomass.

<sup>c</sup> Percentage of carbon in belowground biomass.

*Statistical analyses.* We built linear regression models to estimate total tree carbon content ( $\text{Mg ha}^{-1}$ ) from abiotic and biotic predictors measured at the plot level. To select the group of variables that better explained the total tree carbon, we used a multiple regression analysis with the stepwise forward approximation ( $P < 0.05$  to enter the model). All models reported were tested using the GVLMA package of the R software (Pena and Slate 2006), which does a global validation of linear model assumptions. Also, the  $R^2$ ,  $P$ -value and the relative root mean square error (RRMSE) parameters of the selected models were estimated,

and a Leave-One-Out Cross Validation was performed for the linear models using the Bootstrap package of the R software (Efron and Tibshirani 1993). Partial  $R^2$  was estimated for each variable in the case of multivariate models. All statistical analyses were done with the R statistical software (R Development Core Team 2011).

*Characteristics of plots and modeling scenarios.* Sampling plots were located at a distance from Info between 400 and 5,110 m (table 2). Elevation varied between 11 and 232 m a.s.l., whereas the slopes ranged between 0 and  $46.3^\circ$ . Mo-

**Table 2.** Location and abiotic characteristics of the sampled plots.

Ubicación y características abióticas de las parcelas muestreadas.

Plot	Coordinates Lat/Long	Distance to Info (m)	Elevation (m a.s.l.)	Slope (degrees)	Aspect (northing)	Annual Radiation ( $\text{MJ m}^{-2} \text{ year}^{-1}$ )	Forest condition
1	-43.363705 / -74.112928	650	14	6.3	-0.45	3508	Unburned
2	-43.363399 / -74.107107	940	32	20.9	0.31	3607	Unburned
3	-43.361346 / -74.136485	550	24	13.7	0.96	3767	Unburned
4	-43.358569 / -74.132440	510	11	10.1	-0.61	3437	Unburned
5	-43.352921 / -74.104115	620	46	46.3	0.84	3848	Unburned
6	-43.351325 / -74.107235	400	28	9.3	0.97	3713	Unburned
7	-43.284889 / -74.121162	5110	232	26.0	0.72	3883	Post-fire
8	-43.290648 / -74.117085	4520	181	25.2	-0.97	3098	Post-fire
9	-43.359382 / -74.107018	655	66	28.4	-0.37	3296	Unburned
10	-43.357944 / -74.107360	520	67	39.7	-0.03	3346	Unburned
11	-43.298230 / -74.119453	3660	109	12.0	-0.74	3444	Post-fire
12	-43.302938 / -74.120507	3140	104	5.4	0.26	3590	Post-fire
13	-43.318548 / -74.123402	1460	12	24.8	-0.95	3176	Unburned
14	-43.363710 / -74.111163	740	12	0.0	-0.71	3566	Unburned
Mean <sup>a</sup>			67	8.4	0.11	3514	
SD <sup>a</sup>			66.9	6.9	0.74	245	

<sup>a</sup> Mean and SD were obtained from a 500 m buffer radius that encompassed all the sample points.

deled incident solar radiation varied between 3,098 and 3,883 MJ m<sup>-2</sup> year<sup>-1</sup>. Given the fact that we estimated the Mean ± SD of the variables included in table 2 using a 500 m radius around the plot center points, it is clear that our plots included the extreme values of a 95 % confidence interval. Elevation had a mean ± SD of 67 ± 66.9 m a.s.l, whereas slope was 8.4 ± 6.9° and the solar radiation was 3,514 ± 245MJ m<sup>-2</sup> year<sup>-1</sup>. The northing varied between -0.91 and 0.97.

Tree density seriously varied, between 510 and 3,450 individuals ha<sup>-1</sup> (table 3), which suggested that the plots represented different stages of development of the forest. We used Reineke's model to establish if all plots followed this density-size model, which states that as trees get larger, tree density decreases. We plotted tree density and quadratic mean diameter of each plot (figure 2), together with Reineke's model reported by Gezan *et al.* (2007) for coihue (*Nothofagus dombeyi* (Mirb.) Oerst.). Four plots clearly deviated from the expected value, which coincides with lands previously altered by forest fires; therefore a low density and low quadratic mean diameter is expected. Hereafter we refer to these plots (N° 7, 8, 11, 12) as having a 'post-fire' condition, to differentiate them from the 'unburned' ones (table 2).

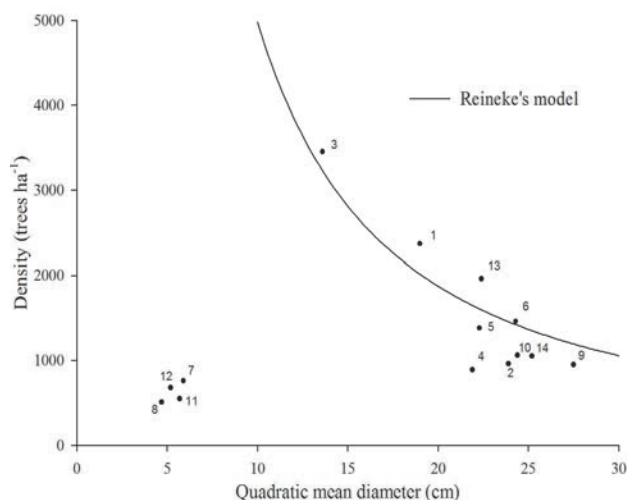


**Figure 2.** Relation between the quadratic mean diameter (QMD) and tree density (D) at each plot. The curve represents the relation reported by Gezan *et al.* (2007) for *N. dombeyi* ( $D = e^{11.7630} * CMD^{-1.4112}$ ). The identification number of each plot is included in the graph.

Relación del diámetro cuadrático medio (QMD) con la densidad de árboles (D) en cada parcela. La línea representa la relación reportada por Gezan *et al.* (2007) para *N. dombeyi* ( $D = e^{11.7630} * CMD^{-1.4112}$ ). La identificación del número de la parcela se incluye en el gráfico.

**Table 3.** Tree density (individuals per hectare) for the species found in the sampled plots.<sup>a</sup>  
 Densidad (individuos ha<sup>-1</sup>) de las especies arbóreas presentes en las parcelas muestreadas.<sup>a</sup>

Plot	Nn	Dw	Am	Lp	Ts	Cp	Pn	Al	Wt	Pl	Ap	La	Lf	Ec	Total	G <sup>c</sup>
1	90	320	10	70	1,640	70	40	120	0	10	0	0	0	0	2,370	88.9
2	420	160	10	0	100	130	0	40	20	50	20	0	0	10	960	49.2
3	190	3,130	20	0	80	30	0	0	0	0	0	0	0	0	3,450	53.5
4	130	590	60	0	20	70	0	20	0	0	0	0	0	0	890	36.4
5	140	70	730	340	0	100	0	0	0	0	0	0	0	0	1,380	56.2
6	80	480	500	360	0	30	10	0	0	0	0	0	0	0	1,460	68.4
7 <sup>b</sup>	360	230	0	0	120	10	0	0	40	0	0	0	0	0	760	2.0
8 <sup>b</sup>	140	20	0	0	140	0	0	0	210	0	0	0	0	0	510	0.9
9	10	210	620	80	0	30	0	0	0	0	0	0	0	0	950	57.5
10	30	280	390	310	0	50	0	0	0	0	0	0	0	0	1,060	51.3
11 <sup>b</sup>	80	160	0	0	90	20	10	0	100	0	0	0	70	20	550	1.7
12 <sup>b</sup>	350	70	10	0	80	20	0	0	140	0	0	0	10	0	680	1.6
13	40	680	950	50	0	200	20	0	0	0	0	20	0	0	1,960	78.6
14	90	300	150	510	0	0	0	0	0	0	0	0	0	0	1,050	58.5
Mean	154	479	246	123	162	54	6	13	36	4	1	1	6	2	1,288	43.2
SE	130	787	87	47	114	15	11	32	17	3	1	1	5	1	217	8

<sup>a</sup> Nn: *N. nitida*; Dw: *D. winteri*; Am: *A. meli*; Lp: *L. philippiana*; Ts: *T. stipularis*; Cp: *C. paniculada*; Pn: *P. nubigenus*; Al: *A. luma*; Wt: *W. trichosperma*; Pl: *P. laetevirens* (Gay) Franch.; Ap: *A. punctatum*; La; *L. apiculata*; Lf: *Lomatia ferruginea*; Ec: *Embothrium coccineum* J.R. Forst. et G. Forst.

<sup>b</sup> Post-fire condition plots.

<sup>c</sup> Basal area (m<sup>2</sup> ha<sup>-1</sup>).

A total of 14 tree species were identified in the sampled plots (table 3). Only *N. nitida* and *D. winteri* had a 100 % frequency, whereas *Amomyrtus meli* (Phil.) D. Legrand *et* Kausel and *C. paniculata* were found in 78.6 and 85.7 % of the sampled plots, respectively. On the contrary, *Luma apiculata* (DC.) Burret and *Aextoxicon punctatum* (Ruiz *et* Pav.) were only found in one of the plots. Floristic composition varied among plots, although *N. nitida* and *D. winteri* were present in all of them and usually very abundant (table 3). In the post-fire condition, *W. trichosperma* and tepú (*Tepualia stipularis* (Hook. *et* Arn.) Griseb.) were among the most frequent species, although in the unburned sites, *L. philippiana*, *A. meli* and *C. paniculata* showed relatively high density.

For these reasons we generated two scenarios for the analyses of tree carbon and its relationship with abiotic and biotic variables: A, excluding the four post-fire plots (N = 10); and B, considering all the plots (N = 14). Additionally, because there was one plot showing an extremely high tree carbon content, we generated a third scenario (C), excluding this one plot (N = 13).

## RESULTS

**Total and species-specific carbon content.** Total carbon content in the above and belowground tree biomass varied between 5.5 and 1,408 Mg ha<sup>-1</sup> (table 4). The average carbon content of the sites affected by fire was 7.7 Mg ha<sup>-1</sup>, while for the non-affected sites the carbon content was in average 384.4 Mg ha<sup>-1</sup>. These two values are not statistically different ( $P = 0.08$ ) given that the carbon content of plot 13 (1,408 Mg ha<sup>-1</sup>) makes the variability very high (SE = 120 Mg ha<sup>-1</sup>). If this plot is removed from the analyses, the average of the unburned plots goes down to 189.7 Mg ha<sup>-1</sup>, being significantly higher than that from the post-fire condition plots ( $P = 0.002$ ).

In terms of individual contribution of tree species to the carbon stock, the major contribution was made by *N. nitida* (figure 3). Only in two of the 14 sampled plots, the major contribution to the carbon stock was made by *D. winteri*. A significant contribution to carbon stocks was also made by *L. philippiana*, *T. stipularis*, and *A. meli* in some of the sampled plots (N° 5, 10, and 14). The contribution of the other tree species to the carbon stock (as a group) was lower than 4 %.

**Modeling total carbon using abiotic and biotic variables.** Table 5 shows the simple and multiple regression analyses that significantly explained total carbon of tree biomass, for the three analysis scenarios. In scenario A (excluding the post-fire plots), the distance to Iníó had a significant effect on total tree carbon content. The distance was also the only variable selected with the stepwise procedure run with abiotic variables, with  $R^2_{adj} = 0.54$ . In scenario B (including all the plots), only the biotic variables showed a significant effect on total tree carbon content, and carbon of *N. nitida* was the variable that had the highest  $R^2_{adj}$  (0.96)

**Table 4.** Species-specific and total carbon content (Mg ha<sup>-1</sup>) in tree biomass (above and belowground), separated by forest condition.<sup>a</sup>

Carbono por especie y total de la biomasa arbórea (Mg ha<sup>-1</sup>), diferenciados por la condición del bosque.<sup>a</sup>

Forest condition	Plot	Nn	Dw	CT
Post-fire	8	1.9	0.3	5.5
	11	1.5	1.9	7.8
	7	4.3	3.3	8.7
	12	4.4	1.2	8.9
Mean ± SE				7.7 ± 0.78
Unburned	4	29.8	61.4	96.6
	2	101.1	18.7	170.3
	14	20.7	72.8	179.4
	5	49.5	34.3	202.2
	10	167.5	16.4	249.4
	3	149.5	114.9	260.6
	9	232.0	60.7	366.5
	1	211.4	25.6	421.9
	6	382.9	57.1	488.6
	13	1349.5	52.0	1408.1
Mean ± SE				384.4 ± 120

<sup>a</sup>Nn, *N. nitida*; Dw, *D. winteri*; CT, total tree carbon in the plot;

(table 5). The model of *N. nitida* was slightly improved when adding the density of all trees ( $R^2_{adj}$  0.97; partial  $R^2$  of *N. nitida* 0.98, partial  $R^2$  of density 0.34). In scenario C (excluding plot 13) a higher number of variables showed significant relation with the total tree carbon, but carbon of *N. nitida* and overall density collectively predicted total carbon with highest power ( $R^2_{adj} = 0.88$ ; table 5) (Partial  $R^2$  were 0.88 for *N. nitida* and 0.25 for density).

In terms of the spectral variables derived from satellite images, only the GreenIndex had a significant contribution to total carbon modeling. Using the stepwise process, the model generated with this index (together with the distance to Iníó) gave an  $R^2_{adj}$  of 0.69 (Partial  $R^2$  were 0.56 for Distance to Iníó and 0.44 for Greenindex) (table 5). Elevation showed a significant inverse effect only in this modeling scenario (C).

Of the biotic variables, tree density had a quadratic effect in scenarios A and C (table 5). The carbon content of individual tree species could only be considered in the case of *D. winteri* and *N. nitida* because they were present in all the plots. The carbon content of *D. winteri* was significant only on scenario C, whereas the carbon content of *N. nitida* had a significant relation with the total tree carbon stock in all the modeling scenarios (table 5), even when all the plots were included (scenario B) (figure 4).

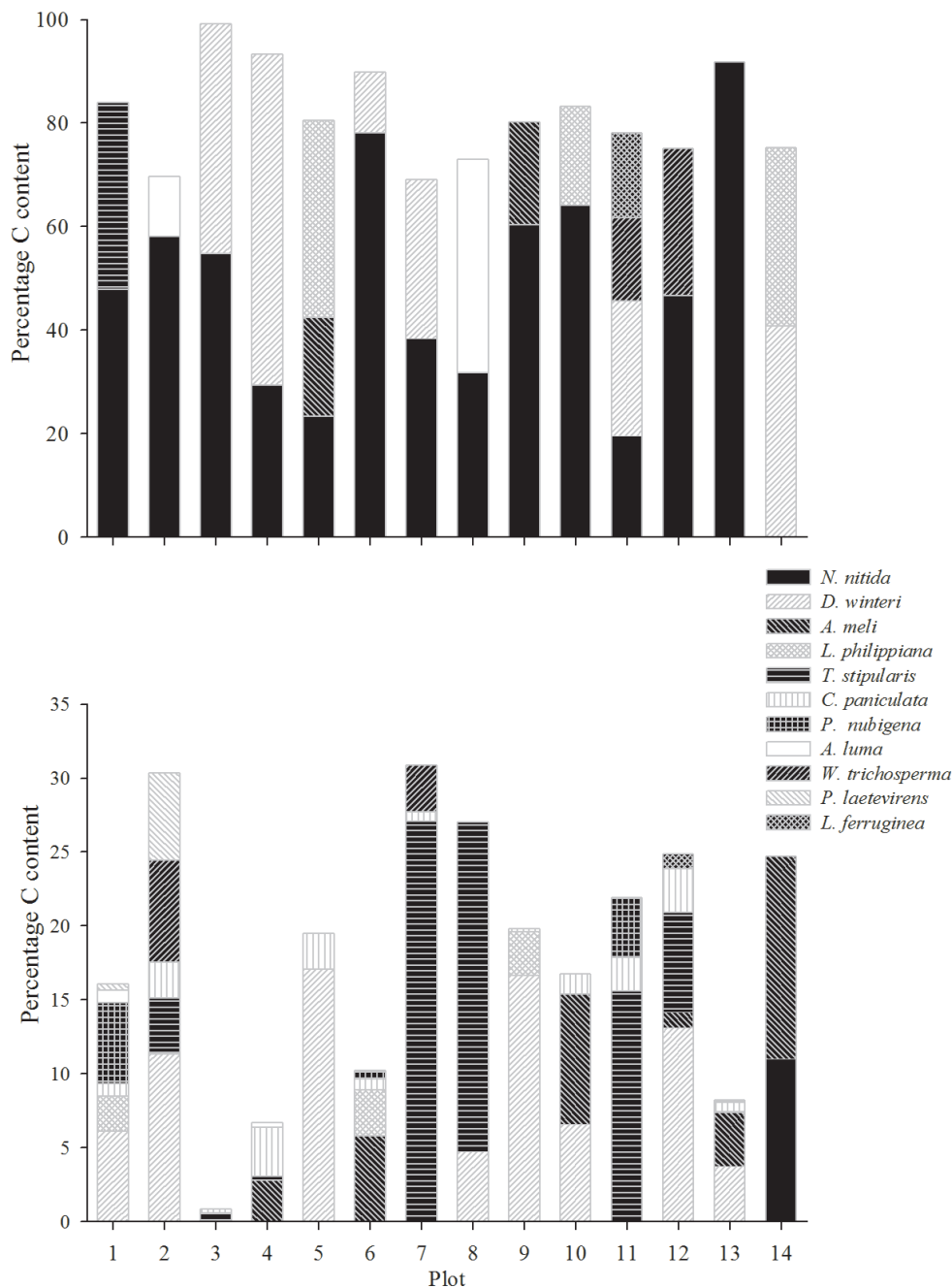


**Figure 3.** Contribution (%) of each species to the total tree carbon stock. The top graph shows the contribution of the two or three species that sum 65 % or more; the bottom graph shows the contribution of the rest of the species. The post-fire plots are 7, 8, 11 and 12.

Contribución porcentual de carbono por especie en cada parcela. El gráfico superior muestra la contribución de las dos o tres especies que suman 65 % o más; el gráfico inferior muestra la contribución del resto de las especies. Las parcelas incendiadas son 7, 8, 11 y 12.

## DISCUSSION

We found large variability of tree species composition and tree carbon content among the sampled plots, which suggested that they represent different successional stages. In general, biotic variables showed a better predictive value of the total tree carbon stock.

We used five specific allometric functions and a general function for the rest of the species present in our study, which were proposed by Gayoso *et al.* (2002) (table 1) to estimate total carbon. The only allometric model that we found in literature specifically built in Chiloé was reported by Naulin (2002) for *D. winteri* (DBH range: 7 - 32 cm). We used the DBH data from Naulin (2002) to test the agre-

**Table 5.** Simple and multiple regression models for estimating the total tree carbon (CT) based on abiotic and biotic variables, for scenarios A (excluding the post-fire condition plots, N =10), B (including all the plots, N =14) and C (excluding plot 13, N =13).<sup>a</sup>

Modelos de regresión simples y múltiples para estimar carbono arbóreo total (CT), basado en variables abióticas y bióticas para los escenarios A (excluyendo las parcelas con condición post-incendio, N=10), B (con todas las parcelas, N=14) y C (excluyendo la parcela 13, N=13).<sup>a</sup>

Variables	Model	R <sup>2</sup> _adj	P	RRMSE (%)	R <sup>2</sup> _LOOCV
Scenario A					
Elevation (A)	-	-	-	-	-
Distance to Iníó (DI)	-294.4 + 0.96 DI	0.54	0.009	59.8	0.33
Stepwise abiotic	-294.4 + 0.96 DI	0.54	0.009	59.8	0.33
Density (D)	-0.001 + 1.73 D -0.0004 D <sup>2</sup>	0.31	0.11	68.8	-
<i>C. D. winteri</i> (CDw)	-	-	-	-	-
<i>C. N. nitida</i> (CNn)	127.29 + 0.954 CNn	0.98	<0.001	11.2	0.98
Stepwise biotic	127.29 + 0.954 CNn	0.98	<0.001	11.2	0.98
Scenario B					
Elevation (A)	-	-	-	-	-
Distance to Iníó (DI)	-	-	-	-	-
Stepwise abiotic	-	-	-	-	-
Density (D)	-	-	-	-	-
<i>C. D. winteri</i> (CDw)	-	-	-	-	-
<i>C. N. nitida</i> (CNn)	81.1 + 1.01 CNn	0.96	<0.001	22.9	0.94
Stepwise biotic	27.03 + 0.971 CNn +0.048 D	0.97	<0.001	19	0.94
Scenario C					
Elevation (A)	297.19 -1.51 A	0.34	0.0203	64.5	0.25
Distance to Iníó (DI)	311.466 - 0.072 DI	0.54	0.0026	54.3	0.45
Stepwise abiotic	81.97 - 0.054 DI + 1259.84 GI <sup>b</sup>	0.69	0.001	42.8	0.65
Density (D)	-0.035 + 0.701 D - 0.0002 D <sup>2</sup>	0.67	0.001	43.5	-
<i>C. D. winteri</i> (CDw)	103.84 + 2.383 CDw	0.19	0.07	71.8	0.07
<i>C. N. nitida</i> (CNn)	53.968 + 1.301 CNn	0.86	<0.001	29.4	0.81
Stepwise biotic	20.68 + 1.188 CNn +0.036 D	0.88	<0.001	26.1	0.76

<sup>a</sup> RRMSE, relative root mean square error; R<sup>2</sup>\_LOOCV, R<sup>2</sup> estimated with Leave-One-Out Cross Validation (it applies only to linear models);

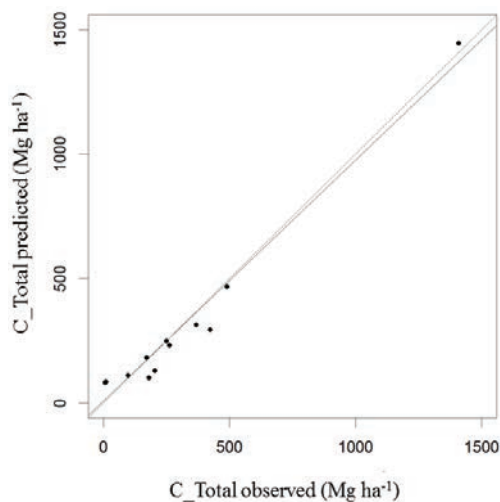


**Figure 4.** Observed vs. predicted total tree carbon for the 14 sampled plots, based on the carbon of *N. nitida*.

Carbono total observado vs predicho, para las 14 parcelas muestreadas, basado en el carbono de *N. nitida*.

ement between her model and Gayoso *et al.*'s and the result was an almost perfect linear relation (slope = 1.0053, R<sup>2</sup> = 0.98, N = 15). This suggests that using the models of Gayoso *et al.* (2002) in Chiloé in other areas is reasonable, having the advantage that their models cover a wider range of DBH (*e.g.*, for *D. winteri* model, DBH range: 6 - 52 cm).

The abiotic variables showed a low predictive value of total tree carbon. Significant models showed that a larger total tree carbon was related to lower altitudes and higher distances to Iníó (table 5), although the latter result applied only when we removed the burned sites, which happened to be located farther from the village (table 1). Total solar radiation did not have a good predictive value, possibly due to the low variation in topography in the study area, as a result of low variability in altitude (11-232 m) and slopes (0-46.3°), which in turn generated a low variation in annual solar radiation (3,098 - 3,883 MJ m<sup>-2</sup> year<sup>-1</sup>). Kumar *et al.* (1997) for example found a broader range of annual solar radiation for a site located at latitude 36° south (3647 - 11,253 MJ m<sup>-2</sup> year<sup>-1</sup>), with similar variation

in slope (0-40°) but higher variation in altitude (90-800 m). If we consider that the calculations of incident radiation include shortwave radiation only, the effects of highly frequent cloudy days in our study area should further decrease the expected effect of latitude and slope on solar radiation.

Despite the fact that various studies have demonstrated the importance of satellite images in biomass modeling (Zheng *et al.* 2004, Labrecque *et al.* 2006, Ji *et al.* 2012), the spectral characterization of satellite images was not relevant in this study. A potential explanation would be linked to the floristic composition of the studied sites, where *N. nitida* is the tree species that defines the total biomass of the forest. Spectral indexes are based in the spectral response of vegetation between the red and near infrared wavebands. With the high levels of biomass in the studied sites, there is a high probability that conventional spectral indexes were saturated, thereby impeding the detection of spectral differences (Hobbs 1995). The GreenIndex, derived from the red and green reflectance, was the only spectral variable that showed a significant statistical relation with the tree carbon stock. A possible explanation

is because it considers the green spectrum instead of the near infrared band in the index formulation. According to Gitelson *et al.* (2010), in order to detect changes based on reflectance measurements in dense canopies, the normalization considering the green band instead of the near infrared band (used in the other indices), should be more sensitive to detect changes in reflectance, allowing a better discrimination of vegetation conditions related to the chlorophyll activity. Further studies should consider the use of remote sensing techniques capable of estimating more detailed spectral information, such as hyperspectral sensors or vertical information of the vegetation (*e.g.*, LiDAR sensors). In this regard, several studies have predicted total biomass estimation with acceptable accuracies (Koch 2010, Gleason and Im 2012). In our case, an issue that may have influenced in the low predictive value of the spectral indices is the confounding effect of dead biomass on the spectral signature of the forest stands.

The high contribution of *N. nitida* to the total tree carbon content when considering all the plots ( $R^2_{adj} = 0.96$ ) implies that the most simple and practical model for total tree carbon determination would only require determining

**Table 6.** Comparison of carbon stock estimated in this study for each forest condition with other forest types.

Comparación del contenido de carbono estimado en este estudio para cada condición del bosque con otros tipos de bosque.

Forest type	Carbon stock (Mg ha <sup>-1</sup> ) <sup>a</sup>	Source
Evergreen broadleaf post-fire (Chile)	7.7	This study
Boreal in slope (Canada)	81.4	Hazlett <i>et al.</i> , (2005)
Boreal riparian (Canada)	83.8	Hazlett <i>et al.</i> (2005)
Coniferous forest in areas surrounding parks (Canada)	76.8 (32 %)	Sharma <i>et al.</i> (2013)
Pine-oak degraded (Mexico)	87.5 (54 %)	Ordoñez <i>et al.</i> (2008)
Coniferous forest in parks (Canada)	101.7 (36 %)	Sharma <i>et al.</i> (2013)
Rainforest Tucuman Bolivian (Argentina)	107.1 (58 %)	Gasparri y Manghi (2004)
Oak (Mexico)	112.8 (79 %)	Ordoñez <i>et al.</i> (2008)
Pine-oak (Mexico)	115.7 (53 %)	Ordoñez <i>et al.</i> (2008)
Pine (Mexico)	126.8 (57 %)	Ordoñez <i>et al.</i> (2008)
Fir (Mexico)	134.5 (79 %)	Ordoñez <i>et al.</i> (2008)
Rainforest Misiones (Argentina)	165.1 (72 %)	Gasparri y Manghi (2004)
Evergreen broadleaf (Chile) <sup>b</sup>	189.7	This study
Mixed evergreen forest (Chile)	250.0 (68 %)	Vann <i>et al.</i> (2002)
European beech (Spain)	293.0 (77 %)	Merino <i>et al.</i> (2007)
Andean Patagonian (Argentina)	334.9 (69 %)	Gasparri y Manghi (2004)
Lowland podocarp-broadleaved (New Zealand)	339.8	Tate <i>et al.</i> (1997)
Evergreen broadleaf unburned (Chile)	384.4	This study

<sup>a</sup> In parenthesis, the percentage of total carbon stored in live-tree biomass.

<sup>b</sup> This is the mean value after excluding one plot with extremely high tree carbon content.

DBH of this species, which holds true even in the post-fire plots. The contribution of *N. nitida* is better appreciated in the sites with high tree carbon content, which represent forest stages near maturity (old growth), where mature individuals (high DBH and biomass) of *N. nitida* occupy a dominant canopy position.

Total tree carbon stock in the unburned sites (table 4) was in the range reported in literature for different types of forest ecosystems (table 6). The only exception to this trend was found in plot 13 that contained 1,408 Mg ha<sup>-1</sup> of carbon. This unexpected high value is due to the presence of two *N. nitida* individuals with DBH around 140 cm; these two trees accounted for 90 % of the total carbon stock of the sampling plot (figure 3). For comparison purposes, we estimated the total tree carbon separately for those plots that did not have a fire history (N = 10), the second set considered all the remaining plots (N = 14) and the third excluded one plot because of its high carbon content (N = 13); total carbon contents were in average ( $\pm$  standard deviation) 7.7  $\pm$  0.78, 384.4  $\pm$  120, 189.7  $\pm$  45.6 Mg ha<sup>-1</sup>, respectively. When the elevated carbon content of one plot was excluded from the analyses, the mean total carbon content was still high when compared with the forest ecosystems that we reviewed and very similar to what Vann *et al.* (2002) reported for a forest in Chiloé island (table 6). The tree carbon stock represents between 32 % and 79 % of the total carbon stored in the forest ecosystems (table 6). The evergreen forests of Chiloé have an elevated carbon storage capacity; thereby their conservation is highly relevant. More detailed studies about the other carbon storage reservoirs (*i.e.* soils, understory and necromass) will contribute to a better understanding of carbon storage and dynamics in these ecosystems.

#### ACKNOWLEDGEMENTS

The authors thank Carlos Oyarzún, Gonzalo Olguín and Constanza Urresty for their help with the field work, the Tantauco Park administration and people from Info for their collaboration and hospitality during the field campaign. Also, we would like to thank the three anonymous reviewers that helped us to improve our manuscript.

#### REFERENCES

- Altamirano A, A Lara. 2010. Deforestation in temperate ecosystems of pre-Andean range of south-central Chile. *Bosque* 31(1): 53-64.
- Ajtay GL, P Ketner, P Duvigneaud. 1979. Terrestrial primary production and phytomass. In Bolin B, E Degens, S Kempe, P Ketner eds. The Global Carbon Cycle. SCOPE edn., Vol. 13. Chichester, USA. Wiley. p. 129-182.
- Brown S. 2002. Measuring carbon in forests: current status and future challenges. *Environment Pollution* 116: 363-372.
- Cajander AK 1926. The theory of forests types. *Acta Forestalia Fennica* 29: 1-108.
- Castillo SM, SR Garfias, AG Julio, RL Gonzalez. 2012. Analysis of large forest fires on native Chilean vegetation. *Interciencia* 37: 796-804.
- Chander G, BL Markham, DL Helder. 2009. Summary of current radiometric calibration coefficients for Landsat MSS, TM, ETM+, and EO-1 ALI Sensors. *Remote Sensing of Environment* 113: 893-903.
- Chavez Jr PS. 1988. An improved dark-object subtraction technique for atmospheric scattering correction of multispectral data. *Remote Sensing of Environment* 24: 459-479.
- CONAMA (Comisión Nacional de Medio Ambiente, CL). 2002. Estrategia Regional para la conservación y utilización sostenible de la biodiversidad, Décima Región de Los Lagos. 156 p.
- Coops N, M Johnson, M Wulder, J White. 2006. Assessment of QuickBird high spatial resolution imagery to detect red attack damage due to mountain pine beetle infestation. *Remote Sensing of Environment* 30: 69-76.
- Corporación Chile Ambiente. 2005. Plan de Acción Parque Tantauco. Santiago, Chile. Corporación Chile Ambiente. 191 p.
- Crist EP, RC Cicone. 1984. A physically-based transformation of Thematic Mapper data - the TM Tasseled Cap. *IEEE Trans. on Geosciences and Remote Sensing* 22: 256-263.
- Donoso C. 1981. Tipos forestales de los bosques nativos de Chile. Documento de trabajo N°38. Investigación y Desarrollo Forestal. Santiago, Chile. CONAF-FAO. 70 p.
- Efron B, R Tibshirani. 1993. An Introduction to the Bootstrap. New York, USA. Chapman and Hall. 456 p.
- Gajardo R. 1994. La vegetación natural de Chile. Clasificación y distribución geográfica. Santiago, Chile. Editorial Universitaria. 165 p.
- Gasparri I, E Manghi. 2004. Estimación de volumen, biomasa y contenido de carbono de las regiones forestales argentinas. Visited 5 dic. 2008. Available in: [www.ambiente.gov.ar/archivos/web/UMSEF/File/volumen\\_biomasa\\_carbono.pdf](http://www.ambiente.gov.ar/archivos/web/UMSEF/File/volumen_biomasa_carbono.pdf).
- Gayoso J, J Guerra, D Alarcón. 2002. Contenido de carbono y funciones de biomasa en especies nativas y exóticas. Informe Proyecto FONDEF D9811076. Valdivia, Chile. Universidad Austral de Chile. 157 p.
- Gezan SA, A Ortega, E Andenmatten. 2007. Diagramas de manejo de densidad para renovales de roble, raulí y coigüe en Chile. *Bosque* 28(2): 97-105.
- Gitelson A, Y Kaufman, R Stark and D Rundquist. 2002. Novel algorithms for remote estimation of vegetation fraction. *Remote Sensing of Environment* 80: 76-87.
- Gleason CJ, J Im. 2012. Forest biomass estimation from airborne LiDAR data using machine learning approaches. *Remote Sensing of Environment* 125:80-91.
- Goodale CL, MJ Apps, RA Birdsey, CB Field, LS Heath, RA Houghton, JC Jenkins, GH Kohlmaier, W Kurz, S Liu, G-J Nabuurs, S Nilsson, AZ Shvidenko. 2002. Forest carbon sinks in the northern hemisphere. *Ecological Applications* 12:891-99.
- Gutiérrez AG, A Huth. 2012. Successional stages of primary temperate rainforests of Chiloé Island, Chile. *Perspectives in Plant Ecology, Evolution and Systematics* 14: 243-256.
- Hazlett PW, AM Gordon, PK Sibley, JM Buttle. 2005. Stand carbon stocks and soil carbon and nitrogen storage for riparian and upland forests of boreal lakes in northeastern Ontario. *Forest Ecology and Management* 219: 56-68.
- Hobbs T. 1995. The use of NOAA-AVHRR NDVI data to assess herbage production in the arid rangelands of Central Australia.

- lia. *International Journal of Remote Sensing* 16:1289-1302
- IPCC (The Intergovernmental Panel on Climate Change, CH). 1996. Land-use change and forestry. Guidelines for National Green house Gas Inventories: Reference Manual (vol. 5). IPCC (The Intergovernmental Panel on Climate Change, CH). 2000. Land Use, Land-Use Change and Forestry. Cambridge University Press. 375 p.
- IPCC (The Intergovernmental Panel on Climate Change, CH). 2007. Climate change 2007: The physical science basis. 77 p.
- Ji L, BK Wylie, DR Noss, B Peterson, MP Waldrop, JW McFarland, J Rover, TN Hollingsworth. 2012. Estimating above-ground biomass in interior Alaska with Landsat data and field measurements. *International Journal of Applied Earth and Observation and Geoinformation* 18:451-461.
- Kauth RJ, GS Thomas. 1976. The tasseled Cap -- A graphic description of the spectral-temporal development of agricultural crops as seen by LANDSAT. Proceedings of the Symposium on Machine Processing of Remotely Sensed Data. Indiana, USA. Purdue University of West Lafayette. p. 4B-41 to 4B-51.
- Keith H, BG Mackey, DB Lindenmayer. 2009. Re-evaluation of forest biomass carbon stocks and lessons from the world's most carbon-dense forests. *Proceedings of the National Academy of Sciences of the United States of America* 106(28): 11635-11640.
- Kim Phat N, W Knorr, K Sophanarith. 2004. Appropriate measures for conservation of terrestrial carbon stocks - Analysis of trends of forest management in Southeast Asia. *Forest Ecology and Management* 191(1-3): 283-299.
- Koch B. 2010. Status and future of laser scanning, synthetic aperture radar and hyperspectral remote sensing data for forest biomass assessment. *ISPRS Journal of Photogrammetry and Remote Sensing* 65: 581-590.
- Kumar L, Skidmore AK, Knowles E. 1997. Modelling topographic variation in solar radiation in a GIS environment. *International Journal of Geographical Information Science* 11(5): 475-497.
- Labrecque S, RA Fournier, JE Luther, D Piercey. 2006. A comparison of four methods to map biomass from Landsat-TM and inventory data in western Newfoundland. *Forest Ecology and Management* 226: 129-144.
- Lu M. 2006. The potential and challenge of remote sensing-based biomass estimation. *International Journal of Remote Sensing* 27(7): 1297-1328.
- Merino A, C Real, JG Alvarez-Gonzalez, MA Rodríguez-Gutián. 2007. Forest structure and C stocks in natural *Fagus sylvatica* forest in southern Europe: The effects of past management. *Forest Ecology and Management* 250: 206-214.
- Moncrieff JB, Jarvis PG, Valentini R. 2000. Canopy fluxes. In Sala OE, RB Jackson, HA Mooney, RW Howarth eds. *Methods in ecosystem science*. New York, USA. Springer-Verlag. p. 161-180.
- Naulin P. 2002. Estimación de la biomasa en un renoval de canelo (*Drimys winteri* J. R. et Foster) en la comuna de Ancud, Décima Región. Tesis Ingeniero Forestal. Santiago, Chile. Facultad de Ciencias Forestales, Universidad de Chile. 45 p.
- Nemani R, L Pierce, S Running. 1993. Forest ecosystem process at the watershed scale: Sensitivity to remotely-sensed leaf area index estimates. *International Journal of Remote Sensing* 14: 2519-2539.
- Ordoñez JAB, BHJ de Jong, F García-Oliva, FL Aviña, JV Pérez, G Guerrero, R Martínez, O Masera. 2008. Carbon content in vegetation, litter, and soil under 10 different land-use and land-cover classes in the Central Highlands of Michoacan, Mexico. *Forest Ecology and Management* 255: 2074-2084.
- Pena EA, EH Slate. 2006. Global Validation of Linear Model Assumptions. *Journal of the American Statistical Association* 101: 341-354.
- R Development Core Team. 2011. R: A language and environment for statistical computing. R Foundation for Statistical Computing, Vienna, Austria. ISBN 3-900051-07-0, URL <http://www.R-project.org/>
- Rouse JW, RH Haas, JA Schell, DW Deering. 1973. Monitoring the vernal advancement and retrogradation (green wave effect) of natural vegetation. Prog. Rep. RSC 1978-1, Remote Sensing Center, Texas A&M Univ., College Station. 93 p. (NTIS No. E73-106393).
- Saramuzza P, E Micijevic, G Chander. 2004. SLC gap-filled products, phase one methodology. Landsat Technical Notes. Visited 1 April 2014. Available at [https://landsat.usgs.gov/documents/SLC\\_Gap\\_Fill\\_Methodology.pdf](https://landsat.usgs.gov/documents/SLC_Gap_Fill_Methodology.pdf)
- Scharma T, WA Kurz, G Stinson, MG Pellatt, Q Li. 2013. A 100-year conservation experiment: Impacts on forest carbon stocks and fluxes. *Forest Ecology and Management* 310: 242-255.
- Schimel DS, JI House, KA Hibbard, P Bousquet, P Ciais, P Peylyn, BH Braswell, MJ Apps, D Baker, A Bondeaus, J Canadall, G Churkina, W Cramer, AS Denning, CB Field, P Friedlingstein, C Goodale, M Heimann, RA Houghton, JA Melillo, B Moore, D Murdiyarso, I Noble, SW Pacala, IC Prentice, MR Raupach, PJ Rayer, RJ Scholes, WL Steffen, C Wirth. 2001. Recent patterns and mechanisms of carbon exchange by terrestrial ecosystems. *Nature* 414(6860): 169-172.
- Schulp CJE, G-J Nabuurs, PH Verburg, RW de Waal. 2008. Effect of tree species on carbon stocks in forest floor and mineral soil and implications for soil carbon inventories. *Forest Ecology and Management* 256: 482-490.
- Spencer RD, MA Green, PH Biggs. 1997. Integrating eucalypt forest inventory and GIS in Western Australia. *Photogrammetric Engineering and Remote Sensing* 63: 179-181.
- Squeo FA, RA Estévez, A Stoll, CF Gaymer, L Letelier, L Sierralta. 2012. Towards the creation of an integrated system of protected areas in Chile: achievements and challenges. *Plant Ecology & Diversity* 5(2): 233-243.
- Tate KR, DJ Giltrap, JJ Claydon, PF Newsome, IAE Atkinson, MD Taylor, R Lee. 1997 Organic carbon stocks in New Zealand's terrestrial ecosystems. *Journal of the Royal Society of New Zealand* 27: 315-335.
- Vann DR, A Joshi, C Pérez, AH Johnson, J Frizano, DJ Zarin, JJ Armesto. 2002. Distribution and cycling of C, N, Ca, Mg, K and P in three pristine, old-growth forests in the Cordillera de Piuchué, Chile. *Biogeochemistry* 60: 25-47.
- Vesterdal L, N Clarke, BD Sigurdsson, P Gundersen, Do tree species influence soil carbon stocks in temperate and boreal forests? *Forest Ecology and Management* 309: 4-18.
- Villagrán C, JJ Armesto, R Leiva. 1986. Recolonización postglacial de Chiloé insular: Evidencias basadas en la distribución geográfica y los modelos de dispersión de la flora. *Revista Chilena de Historia Natural* 59:19-39.
- Zheng D, J Rademacher, J Chen, T Crow, M Bresee, J Le Moi-

ne, Ryu S-R. 2004. Estimating aboveground biomass using Landsat 7 ETM+ data across a managed landscape in northern Wisconsin, USA. *Remote Sensing of Environment* 93: 402-411.

Zheng G, JM Chen, QJ Tian, WM Ju, XQ Xi. 2007. Combining remote sensing imagery and forest age inventory for biomass mapping. *Journal of Environmental Management* 85: 616-623.

Recibido: 10.04.14  
Aceptado: 16.12.14

